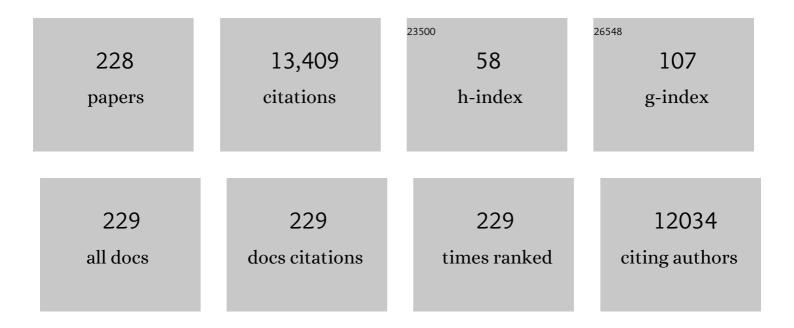
List of Publications by Year in descending order

Source: https://exaly.com/author-pdf/8474037/publications.pdf Version: 2024-02-01



ΖΗΛΝΊΛΟ ΤΛΝ

#	Article	IF	CITATIONS
1	Thermal model of bifacial silicon photovoltaic modules with different backsheets under outdoor conditions. International Journal of Green Energy, 2023, 20, 691-700.	2.1	0
2	Layerâ€byâ€layered organic solar cells: Morphology optimizing strategies and processing techniques. Aggregate, 2022, 3, e107.	5.2	26
3	Recent advances of organometallic complexes in emerging photovoltaics. Journal of Polymer Science, 2022, 60, 865-916.	2.0	23
4	Revival of Insulating Polyethylenimine by Creatively Carbonizing with Perylene into Highly Crystallized Carbon Dots as the Cathode Interlayer for High-Performance Organic Solar Cells. ACS Applied Materials & Interfaces, 2022, 14, 1280-1289.	4.0	19
5	Coordinationâ€Induced Defects Elimination of SnO ₂ Nanoparticles via a Small Electrolyte Molecule for Highâ€Performance Inverted Organic Solar Cells. Advanced Optical Materials, 2022, 10, .	3.6	12
6	Efficient interface modification <i>via</i> multi-site coordination for improved efficiency and stability in organic solar cells. Energy and Environmental Science, 2022, 15, 822-829.	15.6	49
7	Recent Advances of Monolithic <scp>Allâ€Perovskite</scp> Tandem Solar Cells: From Materials to Devices. Chinese Journal of Chemistry, 2022, 40, 856-871.	2.6	11
8	Enhancing the Cycling Stability of Anthraquinone-Based Redox Flow Batteries by Using Thermally Oxidized Carbon Felt. ACS Applied Energy Materials, 2022, 5, 1984-1991.	2.5	14
9	Recent Progress in Semitransparent Organic and Perovskite Solar Cells. Physica Status Solidi (A) Applications and Materials Science, 2022, 219, .	0.8	6
10	Narrowâ€bandwidth emissive carbon dots: A rising star in the fluorescent material family. , 2022, 4, 88-114.		49
11	Noncovalent interactions induced self-association in anthraquinone-iron aqueous redox flow batteries. Sustainable Energy and Fuels, 2022, 6, 2045-2052.	2.5	2
12	Improving charge transport and reducing non-radiative energy loss <i>via</i> a nonacyclic carbazole-based third component for over 18% efficiency polymer solar cells. Journal of Materials Chemistry A, 2022, 10, 7090-7098.	5.2	14
13	Analysis of Electrode Configuration Effects on Mass Transfer and Organic Redox Flow Battery Performance. Industrial & Engineering Chemistry Research, 2022, 61, 2915-2925.	1.8	30
14	Biuret Induced Tinâ€Anchoring and Crystallizationâ€Regulating for Efficient Leadâ€Free Tin Halide Perovskite Lightâ€Emitting Diodes. Small, 2022, 18, e2200036.	5.2	24
15	Interface Modification with CuCrO ₂ Nanocrystals for Highly Efficient and Stable Planar Perovskite Solar Cells. ACS Applied Materials & Interfaces, 2022, 14, 13352-13360.	4.0	15
16	Morphological Stabilization in Organic Solar Cells via a Fluorene-Based Crosslinker for Enhanced Efficiency and Thermal Stability. ACS Applied Materials & Interfaces, 2022, 14, 1187-1194.	4.0	14
17	Recent Advances in Bismuthâ€Based Solar Cells: Fundamentals, Fabrication, and Optimization Strategies. Advanced Sustainable Systems, 2022, 6, .	2.7	8
18	Engineering organic–inorganic perovskite planar heterojunction for efficient carbon dots based light-emitting diodes. Applied Physics Reviews, 2022, 9, .	5.5	7

#	Article	IF	CITATIONS
19	Crosslinkable and Chelatable Organic Ligand Enables Interfaces and Grains Collaborative Passivation for Efficient and Stable Perovskite Solar Cells. Small, 2022, 18, e2201820.	5.2	15
20	Solvent polishing engineering for quasi-two-dimensional perovskite blue light-emitting diodes. Chemical Communications, 2022, 58, 7132-7135.	2.2	6
21	Balance PCE, AVT and CRI for good eye comfort semi-transparent organic photovoltaics via Ga2O3 or In2O3 electron collection layers. Organic Electronics, 2022, , 106572.	1.4	2
22	Selfâ€Assembly Metal Chelate as Ultraviolet Filterable Interface Layer for Efficient Organic Solar Cells. Advanced Energy Materials, 2022, 12, .	10.2	7
23	Battery performance optimization and multi-component transport enhancement of organic flow battery based on channel section reconstruction. Energy, 2022, 258, 124757.	4.5	8
24	Ternary blend strategy in benzotriazole-based organic photovoltaics for indoor application. Green Energy and Environment, 2021, 6, 920-928.	4.7	23
25	Perovskite Passivation Strategies for Efficient and Stable Solar Cells. Solar Rrl, 2021, 5, .	3.1	23
26	Efficient organic solar cells with low-temperature in situ prepared Ga2O3 or In2O3 electron collection layers. Science China Materials, 2021, 64, 1095-1104.	3.5	5
27	High-efficiency red perovskite light-emitting diodes based on collaborative optimization of emission layer and transport layers. Journal of Materials Chemistry C, 2021, 9, 12367-12373.	2.7	16
28	Quadrupole Moment Induced Morphology Control Via a Highly Volatile Small Molecule in Efficient Organic Solar Cells. Advanced Functional Materials, 2021, 31, 2010535.	7.8	55
29	Fluorescent Carbon Dots: Fantastic Electroluminescent Materials for Lightâ€Emitting Diodes. Advanced Science, 2021, 8, 2001977.	5.6	141
30	Recent advances in perovskite/organic integrated solar cells. Rare Metals, 2021, 40, 2763-2777.	3.6	26
31	Highly Efficient and Super Stable Fullâ€Color Quantum Dots Lightâ€Emitting Diodes with Solutionâ€Processed Allâ€Inorganic Charge Transport Layers. Small, 2021, 17, e2007363.	5.2	32
32	Aluminum-Based Surface Polymerization on Carbon Dots with Aggregation-Enhanced Luminescence. Journal of Physical Chemistry Letters, 2021, 12, 4530-4536.	2.1	16
33	Intramolecular hydrogen bonds induced high solubility for efficient and stable anthraquinone based neutral aqueous organic redox flow batteries. Journal of Power Sources, 2021, 498, 229896.	4.0	21
34	pâ€Type Carbon Dots for Effective Surface Optimization for Nearâ€Recordâ€Efficiency CsPbI ₂ Br Solar Cells. Small, 2021, 17, e2102272.	5.2	34
35	Efficient Organic Tandem Solar Cells Enabled by Solutionâ€Processed Interconnection Layer and Fineâ€Tuned Active Layer. Advanced Optical Materials, 2021, 9, 2101246.	3.6	3
36	Realization of high performance for PM6:Y6 based organic photovoltaic cells. Journal of Energy Chemistry, 2021, 61, 29-46.	7.1	54

#	Article	IF	CITATIONS
37	Size-Controllable Metal Chelates as Both Light Scattering Centers and Electron Collection Layer for High-Performance Polymer Solar Cells. CCS Chemistry, 2021, 3, 37-49.	4.6	12
38	Highly efficient carbon dot-based room-temperature fluorescence–phosphorescence dual emitter. Journal of Materials Chemistry C, 2021, 9, 15577-15582.	2.7	15
39	Multiâ€Functional Solid Additive Induced Favorable Vertical Phase Separation and Ordered Molecular Packing for Highly Efficient Layerâ€byâ€Layer Organic Solar Cells. Small, 2021, 17, e2103497.	5.2	49
40	Red Phosphorescent Carbon Quantum Dot Organic Framework-Based Electroluminescent Light-Emitting Diodes Exceeding 5% External Quantum Efficiency. Journal of the American Chemical Society, 2021, 143, 18941-18951.	6.6	54
41	β-Diketone Coordination Strategy for Highly Efficient and Stable Pb–Sn Mixed Perovskite Solar Cells. Journal of Physical Chemistry Letters, 2021, 12, 11772-11778.	2.1	14
42	Strategies Toward Extending the Nearâ€Infrared Photovoltaic Response of Perovskite Solar Cells. Solar Rrl, 2020, 4, 1900280.	3.1	13
43	Microwave-assisted <i>in situ</i> large scale synthesis of a carbon dots@g-C ₃ N ₄ composite phosphor for white light-emitting devices. Materials Chemistry Frontiers, 2020, 4, 517-523.	3.2	34
44	Perylene monoimide and naphthalene-annulated [3,3,3]propellanes: synthesis and device applications. Materials Chemistry Frontiers, 2020, 4, 3539-3545.	3.2	8
45	Diverse applications of MoO ₃ for high performance organic photovoltaics: fundamentals, processes and optimization strategies. Journal of Materials Chemistry A, 2020, 8, 978-1009.	5.2	70
46	Highly efficient ternary polymer solar cells based on a novel double-cabled third component with the same molecular fragments of donor and acceptor moieties. Solar Energy Materials and Solar Cells, 2020, 206, 110326.	3.0	2
47	Lead acetate produced from lead-acid battery for efficient perovskite solar cells. Nano Energy, 2020, 69, 104380.	8.2	30
48	Water-Soluble SnO ₂ Nanoparticles as the Electron Collection Layer for Efficient and Stable Inverted Organic Tandem Solar Cells. ACS Applied Energy Materials, 2020, 3, 12662-12671.	2.5	12
49	Crosslinkable metal chelate as the electron transport layer for efficient and stable inverted polymer solar cells. Materials Chemistry Frontiers, 2020, 4, 2995-3002.	3.2	6
50	High Performance Tandem Solar Cells with Inorganic Perovskite and Organic Conjugated Molecules to Realize Complementary Absorption. Journal of Physical Chemistry Letters, 2020, 11, 9596-9604.	2.1	35
51	A General Approach of Adjusting the Surfaceâ€Free Energy of the Interfacial Layer for Highâ€Performance Organic Solar Cells. Advanced Sustainable Systems, 2020, 4, 2000054.	2.7	14
52	Printable SnO2 cathode interlayer with up to 500 nm thickness-tolerance for high-performance and large-area organic solar cells. Science China Chemistry, 2020, 63, 957-965.	4.2	38
53	Novel cathode buffer layer of Al(acac) ₃ enables efficient, large area and stable semi-transparent organic solar cells. Materials Chemistry Frontiers, 2020, 4, 2072-2080.	3.2	22
54	A co-crystallization induced surface modification strategy with cyanuric acid modulates the bandgap emission of carbon dots. Nanoscale, 2020, 12, 10987-10993.	2.8	46

#	Article	IF	CITATIONS
55	Facile Method of Solvent-Flushing To Building Component Distribution within Photoactive Layers for High-Performance Organic Solar Cells. ACS Applied Materials & Interfaces, 2020, 12, 31459-31466.	4.0	10
56	Recent advances and comprehensive insights on nickel oxide in emerging optoelectronic devices. Sustainable Energy and Fuels, 2020, 4, 4415-4458.	2.5	33
57	High Performance Quasiâ€2D Perovskite Skyâ€Blue Lightâ€Emitting Diodes Using a Dualâ€Ligand Strategy. Small, 2020, 16, e2002940.	5.2	65
58	Deep-blue carbon dots offer high colour purity. Nature Photonics, 2020, 14, 130-131.	15.6	20
59	Efficient Two-Dimensional Tin Halide Perovskite Light-Emitting Diodes via a Spacer Cation Substitution Strategy. Journal of Physical Chemistry Letters, 2020, 11, 1120-1127.	2.1	97
60	High-Efficiency Fluorescence through Bioinspired Supramolecular Self-Assembly. ACS Nano, 2020, 14, 2798-2807.	7.3	49
61	Multifarious Chiral Nanoarchitectures Serving as Handed-Selective Fluorescence Filters for Generating Full-Color Circularly Polarized Luminescence. ACS Nano, 2020, 14, 3208-3218.	7.3	76
62	Self-assembled bulk heterojunctions from integral molecules with nonconjugately linked donor and acceptor units for photovoltaic applications. Sustainable Energy and Fuels, 2020, 4, 3190-3210.	2.5	3
63	Material and device engineering for high-performance blue quantum dot light-emitting diodes. Nanoscale, 2020, 12, 13186-13224.	2.8	57
64	Vertically Oriented BiI ₃ Template Featured BiI ₃ /Polymer Heterojunction for High Photocurrent and Long-Term Stable Solar Cells. ACS Applied Materials & Interfaces, 2019, 11, 32509-32516.	4.0	27
65	Low-temperature in-situ preparation of ZnO electron extraction layer for efficient inverted polymer solar cells. Organic Electronics, 2019, 74, 82-88.	1.4	18
66	Pâ€9.6: Highly Luminescent Blue Quantum Dots Lightâ€Emitting Diodes. Digest of Technical Papers SID International Symposium, 2019, 50, 871-874.	0.1	0
67	Multifunctional pâ€Type Carbon Quantum Dots: a Novel Hole Injection Layer for Highâ€Performance Perovskite Lightâ€Emitting Diodes with Significantly Enhanced Stability. Advanced Optical Materials, 2019, 7, 1901299.	3.6	52
68	Expanding the Light Harvesting of CsPbl ₂ Br to Near Infrared by Integrating with Organic Bulk Heterojunction for Efficient and Stable Solar Cells. ACS Applied Materials & Interfaces, 2019, 11, 37991-37998.	4.0	25
69	Enhancing charge transport in an organic photoactive layer <i>via</i> vertical component engineering for efficient perovskite/organic integrated solar cells. Nanoscale, 2019, 11, 4035-4043.	2.8	22
70	Multifunctional bipyramid-Au@ZnO core–shell nanoparticles as a cathode buffer layer for efficient non-fullerene inverted polymer solar cells with improved near-infrared photoresponse. Journal of Materials Chemistry A, 2019, 7, 2667-2676.	5.2	27
71	Interfacial engineering and optical coupling for multicolored semitransparent inverted organic photovoltaics with a record efficiency of over 12%. Journal of Materials Chemistry A, 2019, 7, 15887-15894.	5.2	83
72	A pentacyclic <i>S</i> , <i>N</i> -heteroacene based electron acceptor with strong near-infrared absorption for efficient organic solar cells. Chemical Communications, 2019, 55, 7057-7060.	2.2	20

#	Article	IF	CITATIONS
73	Electroluminescent Warm White Lightâ€Emitting Diodes Based on Passivation Enabled Bright Red Bandgap Emission Carbon Quantum Dots. Advanced Science, 2019, 6, 1900397.	5.6	174
74	Performance Evaluation of Electron Transport Layers based on PCBM/P3HT BHJ Organic Solar Cells. , 2019, , .		0
75	Achieving Balanced Charge Injection of Blue Quantum Dot Light-Emitting Diodes through Transport Layer Doping Strategies. Journal of Physical Chemistry Letters, 2019, 10, 960-965.	2.1	84
76	Tandem structure: a breakthrough in power conversion efficiency for highly efficient polymer solar cells. Sustainable Energy and Fuels, 2019, 3, 910-934.	2.5	28
77	Highâ€Performance Blue Quantum Dot Lightâ€Emitting Diodes with Balanced Charge Injection. Advanced Electronic Materials, 2019, 5, 1800794.	2.6	34
78	Enhancing the electron blocking ability of n-type MoO3 by doping with p-type NiO for efficient nonfullerene polymer solar cells. Organic Electronics, 2019, 68, 168-175.	1.4	31
79	A Novel Photovoltaic Array Outlier Cleaning Algorithm Based on Sliding Standard Deviation Mutation. Energies, 2019, 12, 4316.	1.6	6
80	Green-solvent-processable strategies for achieving large-scale manufacture of organic photovoltaics. Journal of Materials Chemistry A, 2019, 7, 22826-22847.	5.2	76
81	Semitransparent solar cells with over 12% efficiency based on a new low bandgap fluorinated small molecule acceptor. Materials Chemistry Frontiers, 2019, 3, 2483-2490.	3.2	55
82	Flow characteristics in the containment cooling pools of small modular reactors. International Journal of Heat and Mass Transfer, 2019, 133, 445-460.	2.5	3
83	Passivation of the grain boundaries of CH ₃ NH ₃ PbI ₃ using carbon quantum dots for highly efficient perovskite solar cells with excellent environmental stability. Nanoscale, 2019, 11, 115-124.	2.8	164
84	New Insights into the Formation and Colorâ€Tunable Optical Properties of Multinary Cuâ€Inâ€Znâ€Based Chalcogenide Semiconductor Nanocrystals. Advanced Optical Materials, 2018, 6, 1701389.	3.6	37
85	Engineering the interconnecting layer for efficient inverted tandem polymer solar cells with absorption complementary fullerene and nonfullerene acceptors. Solar Energy Materials and Solar Cells, 2018, 180, 1-9.	3.0	26
86	Boosting photocurrent of GalnP top-cell for current-matched III–V monolithic multiple-junction solar cells via plasmonic decahedral-shaped Au nanoparticles. Solar Energy, 2018, 166, 181-186.	2.9	8
87	Extending absorption of near-infrared wavelength range for high efficiency CIGS solar cell via adjusting energy band. Current Applied Physics, 2018, 18, 484-490.	1.1	31
88	Efficient perovskite/organic integrated solar cells with extended photoresponse to 930 nm and enhanced near-infrared external quantum efficiency of over 50%. Nanoscale, 2018, 10, 3245-3253.	2.8	33
89	Optical–Electrical–Chemical Engineering of PEDOT:PSS by Incorporation of Hydrophobic Nafion for Efficient and Stable Perovskite Solar Cells. ACS Applied Materials & Interfaces, 2018, 10, 3902-3911.	4.0	89
90	Synergy of a titanium chelate electron collection layer and a vertical phase separated photoactive layer for efficient inverted polymer solar cells. Journal of Materials Chemistry A, 2018, 6, 7257-7264.	5.2	20

#	Article	IF	CITATIONS
91	Broadening the Photoresponse to Nearâ€Infrared Region by Cooperating Fullerene and Nonfullerene Acceptors for High Performance Ternary Polymer Solar Cells. Macromolecular Rapid Communications, 2018, 39, 1700492.	2.0	10
92	Solutionâ€Processed Titanium Chelate Used as Both Electrode Modification Layer and Intermediate Layer for Efficient Inverted Tandem Polymer Solar Cells. Chinese Journal of Chemistry, 2018, 36, 194-198.	2.6	19
93	Bright prospect of using alcohol-soluble Nb2O5 as anode buffer layer for efficient polymer solar cells based on fullerene and non-fullerene acceptors. Organic Electronics, 2018, 52, 323-328.	1.4	14
94	All-solution-processed perovskite light-emitting diodes with all metal oxide transport layers. Chemical Communications, 2018, 54, 13283-13286.	2.2	42
95	Manipulating the Tradeâ€off Between Quantum Yield and Electrical Conductivity for Highâ€Brightness Quasiâ€2D Perovskite Lightâ€Emitting Diodes. Advanced Functional Materials, 2018, 28, 1804187.	7.8	113
96	Low-temperature solution-processed vanadium oxide as hole transport layer for efficient and stable perovskite solar cells. Physical Chemistry Chemical Physics, 2018, 20, 21746-21754.	1.3	40
97	Efficient Polymer Solar Cells with Alcohol-Soluble Zirconium(IV) Isopropoxide Cathode Buffer Layer. Energies, 2018, 11, 328.	1.6	6
98	Two-dimensional organic-inorganic hybrid perovskite: from material properties to device applications. Science China Materials, 2018, 61, 1257-1277.	3.5	84
99	Constructing Desired Vertical Component Distribution Within a PBDB-T:ITIC-M Photoactive Layer via Fine-Tuning the Surface Free Energy of a Titanium Chelate Cathode Buffer Layer. Frontiers in Chemistry, 2018, 6, 292.	1.8	21
100	Perfect Complementary in Absorption Spectra with Fullerene, Nonfullerene Acceptors and Medium Band Gap Donor for High-Performance Ternary Polymer Solar Cells. ACS Applied Materials & Interfaces, 2018, 10, 29831-29839.	4.0	15
101	Enhancing the Performance of Blue Quantum Dots Lightâ€Emitting Diodes through Interface Engineering with Deoxyribonucleic Acid. Advanced Optical Materials, 2018, 6, 1800578.	3.6	25
102	Fine Tuning the Light Distribution within the Photoactive Layer by Both Solutionâ€Processed Anode and Cathode Interlayers for High Performance Polymer Solar Cells. Solar Rrl, 2018, 2, 1800141.	3.1	10
103	Engineering triangular carbon quantum dots with unprecedented narrow bandwidth emission for multicolored LEDs. Nature Communications, 2018, 9, 2249.	5.8	676
104	Enhanced Electron Injection and Exciton Confinement for Pure Blue Quantum-Dot Light-Emitting Diodes by Introducing Partially Oxidized Aluminum Cathode. Journal of Visualized Experiments, 2018, , .	0.2	1
105	A Review of the Challenges and Possibilities of Using Carbon Nanotubes in Organic Solar Cells. Science of Advanced Materials, 2018, 10, 747-760.	0.1	15
106	Growing Carbon Quantum Dots for Optoelectronic Devices. Wuli Huaxue Xuebao/ Acta Physico - Chimica Sinica, 2018, 34, 1250-1263.	2.2	13
107	Decahedral-shaped Au nanoparticles as plasmonic centers for high performance polymer solar cells. Organic Electronics, 2017, 43, 33-40.	1.4	24
108	Lightâ€Emitting Diodes: Bright Multicolor Bandgap Fluorescent Carbon Quantum Dots for Electroluminescent Lightâ€Emitting Diodes (Adv. Mater. 3/2017). Advanced Materials, 2017, 29, .	11.1	5

#	Article	IF	CITATIONS
109	Effect of Energy Alignment, Electron Mobility, and Film Morphology of Perylene Diimide Based Polymers as Electron Transport Layer on the Performance of Perovskite Solar Cells. ACS Applied Materials & Interfaces, 2017, 9, 10983-10991.	4.0	76
110	Highly reproducible and uniform SERS substrates based on Ag nanoparticles with optimized size and gap. Photonics and Nanostructures - Fundamentals and Applications, 2017, 23, 58-63.	1.0	17
111	Pure Blue and Highly Luminescent Quantumâ€Dot Lightâ€Emitting Diodes with Enhanced Electron Injection and Exciton Confinement via Partially Oxidized Aluminum Cathode. Advanced Optical Materials, 2017, 5, 1700035.	3.6	39
112	Thiophene–Arylamine Holeâ€Transporting Materials in Perovskite Solar Cells: Substitution Position Effect. Energy Technology, 2017, 5, 1788-1794.	1.8	44
113	Two cyclohexanofullerenes used as electron transport materials in perovskite solar cells. Inorganica Chimica Acta, 2017, 468, 146-151.	1.2	11
114	Tuning driving forces for preparation of faceted single crystalline Au nanoparticles from Au films. Materials Characterization, 2017, 128, 1-6.	1.9	0
115	Engineering the vertical concentration distribution within the polymer:fullerene blends for high performance inverted polymer solar cells. Journal of Materials Chemistry A, 2017, 5, 2319-2327.	5.2	37
116	Tetraphenylmethaneâ€Arylamine Holeâ€Transporting Materials for Perovskite Solar Cells. ChemSusChem, 2017, 10, 968-975.	3.6	45
117	Influence of π-linker on triphenylamine-based hole transporting materials in perovskite solar cells. Dyes and Pigments, 2017, 139, 129-135.	2.0	69
118	Synthesis of highly fluorescent InP/ZnS small-core/thick-shell tetrahedral-shaped quantum dots for blue light-emitting diodes. Journal of Materials Chemistry C, 2017, 5, 8243-8249.	2.7	93
119	Achieving mixed halide perovskite via halogen exchange during vapor-assisted solution process for efficient and stable perovskite solar cells. Organic Electronics, 2017, 50, 33-42.	1.4	23
120	Molecular Engineering of Simple Benzene–Arylamine Hole-Transporting Materials for Perovskite Solar Cells. ACS Applied Materials & Interfaces, 2017, 9, 27657-27663.	4.0	42
121	Enhancing the crystallinity of HC(NH2)2PbI3 film by incorporating methylammonium halide intermediate for efficient and stable perovskite solar cells. Nano Energy, 2017, 40, 248-257.	8.2	72
122	Anthracene–arylamine hole transporting materials for perovskite solar cells. Chemical Communications, 2017, 53, 9558-9561.	2.2	45
123	Efficient and Stable Pure Green All-Inorganic Perovskite CsPbBr ₃ Light-Emitting Diodes with a Solution-Processed NiO _{<i>x</i>} Interlayer. Journal of Physical Chemistry C, 2017, 121, 28132-28138.	1.5	100
124	Incorporating an Electrode Modification Layer with a Vertical Phase Separated Photoactive Layer for Efficient and Stable Inverted Nonfullerene Polymer Solar Cells. ACS Applied Materials & Interfaces, 2017, 9, 43871-43879.	4.0	23
125	Efficient Planar Structured Perovskite Solar Cells with Enhanced Open-Circuit Voltage and Suppressed Charge Recombination Based on a Slow Grown Perovskite Layer from Lead Acetate Precursor. ACS Applied Materials & Interfaces, 2017, 9, 41937-41944.	4.0	23
126	High performance polymer solar cells with electron extraction and light-trapping dual functional cathode interfacial layer. Nano Energy, 2017, 31, 201-209.	8.2	27

#	Article	IF	CITATIONS
127	Bright Multicolor Bandgap Fluorescent Carbon Quantum Dots for Electroluminescent Lightâ€Emitting Diodes. Advanced Materials, 2017, 29, 1604436.	11.1	643
128	The Effect of Donor and Nonfullerene Acceptor Inhomogeneous Distribution within the Photoactive Layer on the Performance of Polymer Solar Cells with Different Device Structures. Polymers, 2017, 9, 571.	2.0	18
129	Blue LEDs: Pure Blue and Highly Luminescent Quantumâ€Dot Lightâ€Emitting Diodes with Enhanced Electron Injection and Exciton Confinement via Partially Oxidized Aluminum Cathode (Advanced) Tj ETQq1 1 0.74	84 3. 1⁄4 rgB	T ¦O verlock
130	Mesoporous TiO2 Nanowire Film for Dye-Sensitized Solar Cell. Journal of Nanoscience and Nanotechnology, 2016, 16, 5605-5610.	0.9	14
131	Diketopyrrolopyrrole or benzodithiophene-arylamine small-molecule hole transporting materials for stable perovskite solar cells. RSC Advances, 2016, 6, 87454-87460.	1.7	26
132	Formulation engineering for optimizing ternary electron acceptors exemplified by isomeric PC ₇₁ BM in planar perovskite solar cells. Journal of Materials Chemistry A, 2016, 4, 18776-18782.	5.2	26
133	Efficient planar perovskite solar cells prepared via a low-pressure vapor-assisted solution process with fullerene/TiO ₂ as an electron collection bilayer. RSC Advances, 2016, 6, 78585-78594.	1.7	27
134	Morphology Engineering for Highâ€Performance and Multicolored Perovskite Lightâ€Emitting Diodes with Simple Device Structures. Small, 2016, 12, 4412-4420.	5.2	125
135	Regular Hexagonal Gold Nanoprisms Fabricated by a Physical Method: Toward Use as Ultrasensitive Surfaceâ€Enhanced Raman Scattering Substrates. Particle and Particle Systems Characterization, 2016, 33, 254-260.	1.2	5
136	Tailoring film agglomeration for preparation of silver nanoparticles with controlled morphology. Materials and Design, 2016, 103, 315-320.	3.3	16
137	Efficient synthesis and photovoltaic properties of highly rigid perylene-embedded benzothiazolyls. Polymer Chemistry, 2016, 7, 780-784.	1.9	15
138	Efficient lead acetate sourced planar heterojunction perovskite solar cells with enhanced substrate coverage via one-step spin-coating. Organic Electronics, 2016, 33, 194-200.	1.4	48
139	The growth of a CH ₃ NH ₃ PbI ₃ thin film using simplified close space sublimation for efficient and large dimensional perovskite solar cells. Energy and Environmental Science, 2016, 9, 1486-1494.	15.6	104
140	Optimization of the Energy Level Alignment between the Photoactive Layer and the Cathode Contact Utilizing Solution-Processed Hafnium Acetylacetonate as Buffer Layer for Efficient Polymer Solar Cells. ACS Applied Materials & Interfaces, 2016, 8, 432-441.	4.0	24
141	Management of the light distribution within the photoactive layer for high performance conventional and inverted polymer solar cells. Journal of Materials Chemistry A, 2016, 4, 1915-1922.	5.2	12
142	Improvement of the power conversion efficiency and long term stability of polymer solar cells by incorporation of amphiphilic Nafion doped PEDOT-PSS as a hole extraction layer. Journal of Materials Chemistry A, 2015, 3, 18727-18734.	5.2	46
143	Efficient perovskite/fullerene planar heterojunction solar cells with enhanced charge extraction and suppressed charge recombination. Nanoscale, 2015, 7, 9771-9778.	2.8	102
144	Performance improvement of conventional and inverted polymer solar cells with hydrophobic fluoropolymer as nonvolatile processing additive. Organic Electronics, 2015, 23, 99-104.	1.4	11

#	Article	IF	CITATIONS
145	Large Optical Nonlinearity Induced by Singlet Fission in Pentacene Films. Angewandte Chemie - International Edition, 2015, 54, 6222-6226.	7.2	24
146	A comparison of n-type copolymers based on cyclopentadithiophene and naphthalene diimide/perylene diimides for all-polymer solar cell applications. Polymer Chemistry, 2015, 6, 7594-7602.	1.9	35
147	Solution-processable metal oxides/chelates as electrode buffer layers for efficient and stable polymer solar cells. Energy and Environmental Science, 2015, 8, 1059-1091.	15.6	265
148	Recent advances in planar heterojunction organic-inorganic hybrid perovskite solar cells. Wuli Xuebao/Acta Physica Sinica, 2015, 64, 038401.	0.2	16
149	Solution-processed nickel compound as hole collection layer for efficient polymer solar cells. Journal Physics D: Applied Physics, 2014, 47, 505101.	1.3	9
150	Effects of Fullerene Bisadduct Regioisomers on Photovoltaic Performance. Advanced Functional Materials, 2014, 24, 158-163.	7.8	104
151	Solutionâ€Processed Rhenium Oxide: A Versatile Anode Buffer Layer for High Performance Polymer Solar Cells with Enhanced Light Harvest. Advanced Energy Materials, 2014, 4, 1300884.	10.2	71
152	Solution-Processed and Low-Temperature Annealed CrO _{<i>x</i>} as Anode Buffer Layer for Efficient Polymer Solar Cells. Journal of Physical Chemistry C, 2014, 118, 9309-9317.	1.5	29
153	Efficient polymer solar cells with a solution-processed and thermal annealing-free RuO ₂ anode buffer layer. Journal of Materials Chemistry A, 2014, 2, 1318-1324.	5.2	64
154	Synthesis, characterization and photovoltaic properties of benzo[1,2-b:4,5-bâ€2]dithiophene-bridged molecules. RSC Advances, 2014, 4, 63260-63267.	1.7	11
155	Trapping Light with a Nanostructured CeO _x /Al Back Electrode for Highâ€Performance Polymer Solar Cells. Advanced Materials Interfaces, 2014, 1, 1400197.	1.9	33
156	Triphenylamine modified bis-diketopyrrolopyrrole molecular donor materials with extended conjugation for bulk heterojunction solar cells. Organic Electronics, 2014, 15, 2575-2586.	1.4	17
157	Nonlinear Density Dependence of Singlet Fission Rate in Tetracene Films. Journal of Physical Chemistry Letters, 2014, 5, 3462-3467.	2.1	19
158	Finding the Lost Open-Circuit Voltage in Polymer Solar Cells by UV-Ozone Treatment of the Nickel Acetate Anode Buffer Layer. ACS Applied Materials & Interfaces, 2014, 6, 9458-9465.	4.0	34
159	High performance polymer solar cells with as-prepared zirconium acetylacetonate film as cathode buffer layer. Scientific Reports, 2014, 4, 4691.	1.6	165
160	Using waterâ€soluble nickel acetate as hole collection layer for stable polymer solar cells. Journal of Applied Polymer Science, 2013, 128, 684-690.	1.3	6
161	[6,6]â€Phenylâ€C ₆₁ â€Butyric Acid Dimethylamino Ester as a Cathode Buffer Layer for Highâ€Performance Polymer Solar Cells. Advanced Energy Materials, 2013, 3, 1569-1574.	10.2	77
162	Construction of Planar and Bulk Integrated Heterojunction Polymer Solar Cells Using Cross-Linkable D-A Copolymer. ACS Applied Materials & Interfaces, 2013, 5, 6591-6597.	4.0	25

#	Article	IF	CITATIONS
163	Stabilization of the film morphology in polymer: Fullerene heterojunction solar cells with photocrosslinkable bromineâ€functionalized lowâ€bandgap copolymers. Journal of Polymer Science Part A, 2013, 51, 3123-3131.	2.5	24
164	A Hyperbranched Conjugated Polymer as the Cathode Interlayer for Highâ€Performance Polymer Solar Cells. Advanced Materials, 2013, 25, 6889-6894.	11.1	101
165	High-Performance Polymer Solar Cells with Solution-Processed and Environmentally Friendly CuO _{<i>x</i>} Anode Buffer Layer. ACS Applied Materials & Interfaces, 2013, 5, 10658-10664.	4.0	77
166	Efficient and stable polymer solar cells with solution-processed molybdenum oxide interfacial layer. Journal of Materials Chemistry A, 2013, 1, 657-664.	5.2	126
167	Significant improvement of photovoltaic performance by embedding thiophene in solution-processed star-shaped TPA-DPP backbone. Journal of Materials Chemistry A, 2013, 1, 5747.	5.2	69
168	Efficient quantum dot light-emitting diodes with solution-processable molybdenum oxide as the anode buffer layer. Nanotechnology, 2013, 24, 175201.	1.3	26
169	Improved performance of polymer solar cells based on P3HT and ICBA using alcohol soluble titanium chelate as electron collection layer. Organic Electronics, 2013, 14, 845-851.	1.4	20
170	Molecular Design toward Efficient Polymer Solar Cells with High Polymer Content. Journal of the American Chemical Society, 2013, 135, 8464-8467.	6.6	86
171	ITO electrode/photoactive layer interface engineering for efficient inverted polymer solar cells based on P3HT and PCBM using a solution-processed titanium chelate. Journal Physics D: Applied Physics, 2012, 45, 285102.	1.3	19
172	Effects of Alkoxy Chain Length in Alkoxy-Substituted Dihydronaphthyl-Based [60]Fullerene Bisadduct Acceptors on Their Photovoltaic Properties. ACS Applied Materials & Interfaces, 2012, 4, 5966-5973.	4.0	27
173	Fine-tuning device performances of small molecule solar cells via the more polarized DPP-attached donor units. Physical Chemistry Chemical Physics, 2012, 14, 14238.	1.3	53
174	Solution-Processed Tungsten Oxide as an Effective Anode Buffer Layer for High-Performance Polymer Solar Cells. Journal of Physical Chemistry C, 2012, 116, 18626-18632.	1.5	157
175	Alcohol soluble titanium(IV) oxide bis(2,4-pentanedionate) as electron collection layer for efficient inverted polymer solar cells. Organic Electronics, 2012, 13, 2429-2435.	1.4	31
176	Synthesis, Characterization, and Electroluminescent Properties of Pyridinylene Vinylene-Modified Phenylene Vinylene Copolymers. Journal of Electronic Materials, 2012, 41, 2447-2452.	1.0	0
177	Solution-processed vanadium oxide as a hole collection layer on an ITO electrode for high-performance polymer solar cells. Physical Chemistry Chemical Physics, 2012, 14, 14589.	1.3	75
178	Dihydronaphthyl-based [60]fullerene bisadducts for efficient and stable polymer solar cells. Chemical Communications, 2012, 48, 425-427.	2.2	122
179	Design, Application, and Morphology Study of a New Photovoltaic Polymer with Strong Aggregation in Solution State. Macromolecules, 2012, 45, 9611-9617.	2.2	664
180	Highly Emissive and Colorâ€Tunable CuInS ₂ â€Based Colloidal Semiconductor Nanocrystals: Offâ€Stoichiometry Effects and Improved Electroluminescence Performance. Advanced Functional Materials, 2012, 22, 2081-2088.	7.8	449

#	Article	IF	CITATIONS
181	Highly Efficient and Thermally Stable Polymer Solar Cells with Dihydronaphthylâ€Based [70]Fullerene Bisadduct Derivative as the Acceptor. Advanced Functional Materials, 2012, 22, 2187-2193.	7.8	104
182	Solution-processed nickel acetate as hole collection layer for polymer solar cells. Physical Chemistry Chemical Physics, 2012, 14, 14217.	1.3	75
183	Highâ€Performance Inverted Polymer Solar Cells with Solutionâ€Processed Titanium Chelate as Electronâ€Collecting Layer on ITO Electrode. Advanced Materials, 2012, 24, 1476-1481.	11.1	305
184	Comparative study of the optical, electrochemical, electrolumiscent, and photovoltaic properties of dendritic pendants modified poly(<i>p</i> â€phenylene vinylene)s. Polymers for Advanced Technologies, 2011, 22, 2503-2508.	1.6	2
185	Nearâ€Bandâ€Edge Electroluminescence from Heavyâ€Metalâ€Free Colloidal Quantum Dots. Advanced Materials, 2011, 23, 3553-3558.	11.1	180
186	Synthesis and photovoltaic properties of polythiophene derivatives with side chains containing C ₆₀ end group. Journal of Applied Polymer Science, 2010, 115, 532-539.	1.3	11
187	Quantum efficiency of stimulated emission in colloidal semiconductor nanocrystal quantum dots. Physical Review B, 2009, 80, .	1.1	8
188	Integration of planar and bulk heterojunctions in polymer/nanocrystal hybrid photovoltaic cells. Applied Physics Letters, 2009, 95, 063510.	1.5	35
189	Colloidal nanocrystal-based light-emitting diodes fabricated on plastic toward flexible quantum dot optoelectronics. Journal of Applied Physics, 2009, 105, .	1.1	43
190	Colloidal nanocrystal-based light-emitting diodes fabricated on plastic - Towards flexible quantum dot optoelectronics. , 2009, , .		0
191	Copolymers of perylene diimide with dithienothiophene and dithienopyrrole as electron-transport materials for all-polymer solar cells and field-effect transistors. Journal of Materials Chemistry, 2009, 19, 5794.	6.7	165
192	Novel twoâ€dimensional donor–acceptor conjugated polymers containing quinoxaline units: Synthesis, characterization, and photovoltaic properties. Journal of Polymer Science Part A, 2008, 46, 4038-4049.	2.5	69
193	A phenylenevinyleneâ€thiopheneâ€phenyleneethynylene copolymer: synthesis, characterization, and photovoltaic properties. Polymers for Advanced Technologies, 2008, 19, 865-871.	1.6	8
194	Electroluminescence and photovoltaic properties of poly(<i>p</i> â€phenylene vinylene) derivatives with dendritic pendants. Journal of Applied Polymer Science, 2008, 107, 514-521.	1.3	25
195	Composition-limited spectral response of hybrid photovoltaic cells containing infrared PbSe nanocrystals. Journal of Applied Physics, 2008, 104, 044306.	1.1	19
196	Stable Binary Complementary White Light-Emitting Diodes Based on Quantum-Dot/Polymer-Bilayer Structures. IEEE Photonics Technology Letters, 2008, 20, 1998-2000.	1.3	32
197	Efficient all-polymer solar cells based on blend of tris(thienylenevinylene)-substituted polythiophene and poly[perylene diimide- <i>alt</i> -bis(dithienothiophene)]. Applied Physics Letters, 2008, 93, .	1.5	123
198	Developing bright and color-saturated quantum dot light emitting diodes towards next generation displays and solid state lighting. , 2008, , .		0

#	Article	IF	CITATIONS
199	Developing Bright and Color-Saturated Quantum Dot Light Emitting Diodes towards Next Generation Displays and Solid State Lighting. , 2008, , .		0
200	Performance improvement of polymer solar cells by using a solution processible titanium chelate as cathode buffer layer. Applied Physics Letters, 2007, 91, 023509.	1.5	64
201	An Electrogenerated Chemical-Oxidation-Driving Nonvolatile Plastic Memory Device with the Conjugated Polymer/Carbon Nanotube Blend. Electrochemical and Solid-State Letters, 2007, 10, P19.	2.2	3
202	Synthesis, optical and electroluminescent properties of an alternating copolymer of triphenylamine and fumaronitrile. Synthetic Metals, 2007, 157, 690-695.	2.1	11
203	Synthesis and Photovoltaic Properties of a Donorâ^'Acceptor Double-Cable Polythiophene with High Content of C60Pendant. Macromolecules, 2007, 40, 1868-1873.	2.2	92
204	Double-Layer Structured WPLEDs Based on Three Primary RGB Luminescent Polymers:  Toward High Luminous Efficiency, Color Purity, and Stability. Journal of Physical Chemistry C, 2007, 111, 6862-6867.	1.5	36
205	Synthesis, Hole Mobility, and Photovoltaic Properties of Cross-Linked Polythiophenes with Vinyleneâ^'Terthiopheneâ^'Vinylene as Conjugated Bridge. Macromolecules, 2007, 40, 1831-1837.	2.2	81
206	A High-Mobility Electron-Transport Polymer with Broad Absorption and Its Use in Field-Effect Transistors and All-Polymer Solar Cells. Journal of the American Chemical Society, 2007, 129, 7246-7247.	6.6	1,110
207	Bright and Color-Saturated Emission from Blue Light-Emitting Diodes Based on Solution-Processed Colloidal Nanocrystal Quantum Dots. Nano Letters, 2007, 7, 3803-3807.	4.5	197
208	Poly(quinoxaline vinylene) With Conjugated Phenylenevinylene Side Chain: A Potential Polymer Acceptor With Broad Absorption Band. Macromolecular Chemistry and Physics, 2007, 208, 1294-1300.	1.1	13
209	White polymer light-emitting diodes based on poly(2-(4′-(diphenylamino)phenylenevinyl)-1,4-phenylene-alt-9,9-n-dihexylfluorene-2,7-diyl) doped with a poly(p-phenylene vinylene) derivative. Thin Solid Films, 2007, 516, 47-51.	0.8	10
210	Synthesis, characterization and photovoltaic properties of thiophene copolymers containing conjugated side-chain. European Polymer Journal, 2007, 43, 855-861.	2.6	18
211	Synthesis and optical properties of fluorene and p-phenylenevinylene copolymers containing non-conjugated spacer. European Polymer Journal, 2007, 43, 1394-1401.	2.6	11
212	Synthesis, characterization, and electroluminescence of new conjugated PPV derivatives bearing triphenylamine side-chain through a vinylene bridge. Polymers for Advanced Technologies, 2007, 18, 963-970.	1.6	5
213	Synthesis, hole mobility, and photovoltaic properties of two alternating poly[3-(hex-1-enyl)thiophene-co-thiophene]s. Journal of Polymer Science Part A, 2007, 45, 629-638.	2.5	33
214	Synthesis and Photovoltaic Properties of Two-Dimensional Conjugated Polythiophenes with Bi(thienylenevinylene) Side Chains. Journal of the American Chemical Society, 2006, 128, 4911-4916.	6.6	759
215	Branched Poly(thienylene vinylene)s with Absorption Spectra Covering the Whole Visible Region. Macromolecules, 2006, 39, 4657-4662.	2.2	125
216	Effect of Branched Conjugation Structure on the Optical, Electrochemical, Hole Mobility, and Photovoltaic Properties of Polythiophenes. Journal of Physical Chemistry B, 2006, 110, 26062-26067.	1.2	69

#	Article	IF	CITATIONS
217	Synthesis of New Conjugated Polyfluorene Derivatives Bearing Triphenylamine Moiety through a Vinylene Bridge and Their Stable Blue Electroluminescence. Chemistry of Materials, 2006, 18, 1053-1061.	3.2	77
218	Thinner-film plastic photovoltaic cells based on different C60 derivatives. Polymers for Advanced Technologies, 2006, 17, 500-505.	1.6	11
219	Effect of side-chain end groups on the optical, electrochemical, and photovoltaic properties of side-chain conjugated polythiophenes. Journal of Polymer Science Part A, 2006, 44, 4916-4922.	2.5	70
220	Linking Polythiophene Chains Through Conjugated Bridges: A Way to Improve Charge Transport in Polymer Solar Cells. Macromolecular Rapid Communications, 2006, 27, 793-798.	2.0	59
221	White light from polymer light-emitting diodes: Utilization of fluorenone defects and exciplex. Applied Physics Letters, 2006, 88, 163510.	1.5	68
222	Synthesis, electroluminescence, and photovoltaic properties of dendronized poly(p-phenylene) Tj ETQq0 0 0 rgBT	/Overlock 1.8	10 Tf 50 54:
223	Morphology and properties of soy protein plastics modified with chitin. Journal of Applied Polymer Science, 2003, 90, 3676-3682.	1.3	57
224	Efficient Hybrid Infrared Solar Cells Based on P3HT and PbSe Nanocrystal Quantum Dots. Materials Science Forum, 0, 685, 38-43.	0.3	3
225	Waterâ€Induced Formation of αâ€MoO 3 Microcrystals as Anode Buffer Layer for Highly Efficient Polymer Solar Cells. Energy Technology, 0, , 2100718.	1.8	1
226	Analysis of photovoltaic system under over-irradiation conditions in arid climate. International Journal of Green Energy, 0, , 1-12.	2.1	1

227	Highâ€Efficiency Microcavity Semitransparent Organic Photovoltaics with Simultaneously Improved Average Visible Transmittance and Color Rendering Index. Solar Rrl, 0, , 2200174.	3.1	8
228	A Lowâ€Potential and Stable Bisâ€Dimethylamino Substituted Anthraquinone for pHâ€Neutral Aqueous Redox Flow Batteries. ChemElectroChem, 0, , .	1.7	4